NOTES ON OCTAHEDRAL IDEAL-TRIANGULATIONS

BIRCH BRYANT

1. Octahedral Decompositions

In [5] Thurston described an ideal-triangulation of $S^3\backslash K \simeq S^3\backslash\overline{N(K)}$, the complement of a knot in the 3-sphere with instructions coming from an oriented diagram of K. See Kim, Kim and Yoon [3] for an easier to locate exposition on this ideal-triangulation. A triangulation $\mathcal{T}$ is a finite collection $\mathbf{\Delta} = \{\Delta_i\}$ of tetrahedra together with a collection $\mathbf{\Phi}$ of isomorphisms between pairs of faces σ_i, σ_j of tetrahedra Δ_k, Δ_l (possible $k = l$). The triangulation is said to be an *ideal-triangulation* of the interior of a compact manifold M with non-empty boundary if the complement of the 0-skeleton in the space created by $\mathcal{T}$ is homeomorphic to $M\backslash\partial M$. These tetrahedra with their vertices removed (truncated) are called *ideal-tetrahedra* and the notions of ideal-octahedra are analogous. The vertices are called *ideal-vertices* and the boundary of a regular neighborhood of an ideal-vertex v is denoted $link(v)$.

Let o be an octahedron. There are, up to symmetry, two ways to triangulate o that appear in the relevant literature, both constructed by adding *central edges* between vertices of the octahedron. The first with four tetrahedra, $o^{(4)}$, and the second with five, $o^{(5)}$. These are shown below in Figure 1, regarding every 3 edge cycle to be a face of a tetrahedron. An ideal-octahedron can be triangulated with ideal-tetrahedra by truncating the tetrahedra of $o^{(4)}$ or $o^{(5)}$. For the remainder of this note we will focus on $o^{(5)}$ and drop the superscript notation. Note that $o^{(4)}$ has many of the same combinatorial properties as $o^{(5)}$.

Let K be a knot in S^3 with diagram D. At a crossing c_i, we call the portion of the knot crossing over (under) the *over-(under-)strand*. At each crossing c_i of D we fix an ideal-octahedron $o_i(012345)$ with "top" (vertex 0) and "bottom" (vertex 5) vertices on the over-strands and under-strands as shown in Figure 2. What one intuitively wants to do is wrap the top and bottom truncated faces around the knot as indicated by the red and green arrows in Figure 2. The literature, particularly [3], achieve this by giving instruction to identify the red edges and green edges. This presents an issue

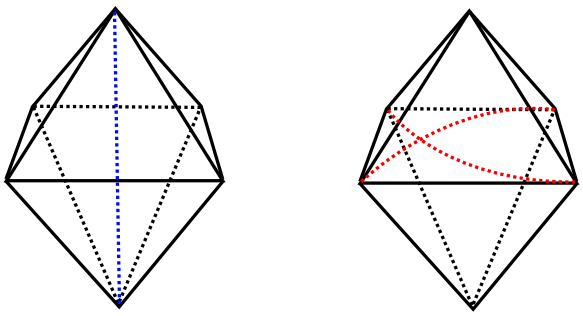


Figure 1. Four and five tetrahedra triangulations of an octahedron

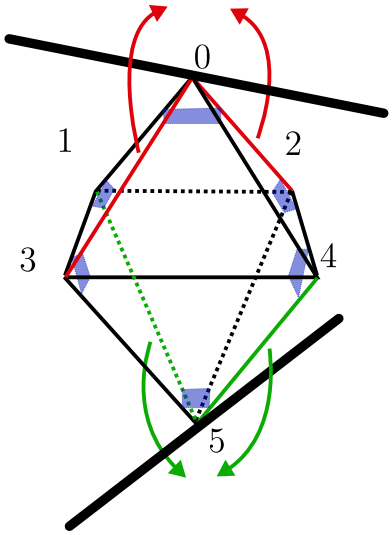


FIGURE 2. Side view of an ideal-octahedron, $o(012345)$, placed between over and under strands.

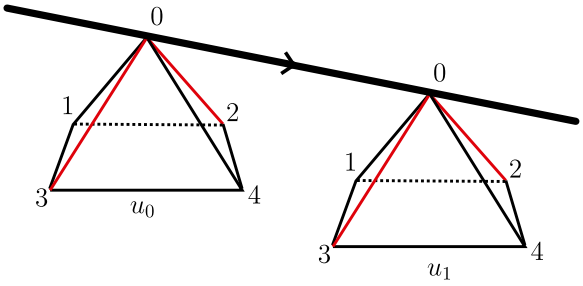


FIGURE 3. The two square pyramids, u_0, u_1, attached to K at consecutive over-strands.

in implementation; as described above, triangulations are formed by face pairings of tetrahedra. There is no mechanism to identify two edges (nor would one be likely to want there to be). We will accomplish this same edge identification through face pairings, simultaneously describing how to identify the ideal-octahedra together to form the first step in our ideal-triangulation.

Recall that we focus here only on the five tetrahedra triangulations of the octahedron o. We will further only consider those whose central edges are not incident to the vertices lying on K. It is then natural to consider o as made from two square pyramids. We now describe how to identify the faces of these pyramids. Let $u_i = o_i(01234), u_i = o_i(01234)$ (possibly $i = j$) be square pyramids incident to consecutive over-strands as in Figure 3. We glue the faces via the vertex identifications as follows: $u_i(034) \to u_j(031), u_i(024) \to u_j(021)$. Similarly if $l_i = o_i(12345), l_j = o_j(12345)$ are square pyramids incident to consecutive under-strands as in Figure 4, we glue the faces via the identifications $l_i(135) \to l_j(125), l_i(345) \to l_j(245)$.

For a sequence of consecutive under-strands and the associated square pyramids $l_i, \dots, l_{i+k}$, the previous face pairing gives a layering of tetrahedra, with the green highlighted edges representing two distinct edge classes $e_0 = l_i(15) = \cdots = l_{i+k}(15)$ and $e_1 = l_i(45) = \cdots = l_{i+k}(45)$. For over-strands we have a similar layering. We

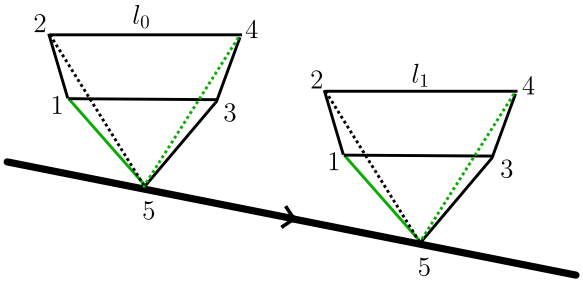


FIGURE 4. The two square pyramids, l_0, l_1, attached to K at consecutive under-strands.

have yet to identify these two green (red) edge classes as described in Figure 2. Suppose now that an over-strand connects into and under-strand and let u_i, l_j be the associated square pyramids as in Figure 6. We make the face pairings $u_i(034) \to l_j(521), u_i(024) \to l_j(524)$. After gluing, the red edges of u_0 in Figure 6 are in the same edge class, likewise are the two green edges of l_1.

So long as there are both over and under crossings for an oriented knot the above face pairings will wrap the edges around the strand as depicted in Figure 2. This is, of course, always the case unless K is the unknot. As we travel along the entirety of the oriented knot, gluing the ideal-octahedra as prescribed above, we will pair every face in the collection $\{o_i\}$ with an orientation reversing map. Thus we have a constructed an ideal-octahedral decomposition $\mathcal{O}$ of some manifold M, it is left to determine M.

Remark 1.1. We have justified the edge identifications given in [3], so we can now rightly view the octahedra as twisted ideal-octahedra shown in Figure 7. The author envisions the twisted ideal-octahedra as beads with two holes through which K is threaded.

The ideal-octahedral decomposition has three vertices: $v_K = \{o_i(0), o_i(5)\}, v_N = \{o_i(2), o_i(3)\}, v_S = \{o_i(1), o_i(4)\}$. The link of v_K is, by design, a torus. See [3, 4] for a schematic on the induced cell decomposition of $link(v_K)$. Now we consider $link(v_N)$. As every face of $\mathcal{O}$ is paired with some other distinct face, the quadrilaterals at the truncated vertices $o_i(2)$ and $o_i(3)$ have their edges identified so that they form a cellular decomposition of the closed surface $link(v_N)$. Suppose the diagram D has C crossings. At each crossing c_i there is a corresponding ideal-octahedron o_i which contributes exactly two quadrilaterals to $link(v_N)$. Thus there are $2C$ faces and $4C$ edges in the cellular decomposition. Finally, above each crossing there is a vertex and above each region of the diagram D on the 2-sphere there is at least one vertex. *Note these two types of vertices as described are never identified!*. As a diagram must have $C + 2$ regions, there are at least $2C + 2$ vertices in the induced cellular decomposition of $link(v_N)$. We can then compute the Euler Characteristic $\chi(link(v_N)) \geq 2C - 4C + 2C + 2 \geq 2$. As $link(v_N)$ is a closed surface, it follows that it must be homeomorphic to a 2-sphere. A similar argument shows $link(v_S) \simeq S^2$.

Remark 1.2. As the link of v_N and v_S are both 2-spheres, $\mathcal{O}$ is in fact an octahedral decomposition of $S^3 \backslash K$ with two "material" vertices and one ideal-vertex lying on the knot K. These mixed type decompositions are very usable, but we continue with the recognition of $\mathcal{O}$.

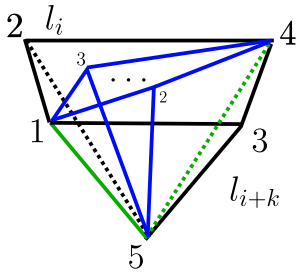


FIGURE 5. Layering of $k+1$ consecutive square pyramids $l_i, \ldots, l_{i+k}$

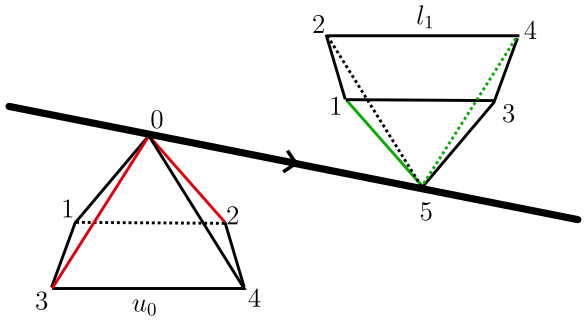


FIGURE 6. Two pyramids, u_0, l_1, attached to K at alternating crossings.

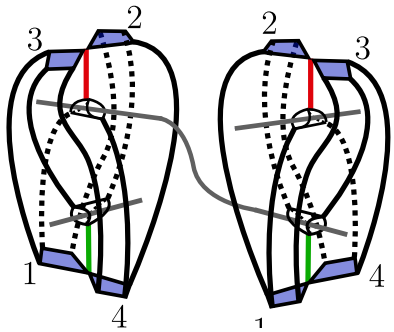


FIGURE 7. Two twisted ideal-octahedron as in [3] with truncated vertices $1, 2, 3, 4$ labeled.

Consider a twisted ideal-octahedron o_i as in Figure 7 with the holes at vertices 0 and 5 filled with 3-balls. Every horizontal cross-section of o_i after filling is either an octagonal disc d_i, or two quads meeting at a single vertex, call the unions ν_i and μ_i, which are isotopic into either $o(2) \cup o(3)$ and $o(1) \cup o(4)$ respectively. The surface S in M represented by identifying the edges of each d_i with identifications induced by the face pairings of $\mathcal{O}$ is a 2-sphere with homeomorphism given by a cell-like map from S to $link(v_N)$ shown in Figure 8.

We finally conclude that M is homeomorphic to $(S^2 \times I) \backslash K$, where we can recover the knot K from the combinatorial information of the ideal-octahedra of $\mathcal{O}$. To form an ideal-triangulation of $S^3 \backslash K$ first triangulate each octahedron of $\mathcal{O}$ to form an ideal-triangulation $\mathcal{T}$ of M. We then drill a tube from $link(v_N)$ to $link(v_K)$ and from $link(v_S)$ to $link(v_K)$. This is achieved by adding "pillows with pre-drilled tube" triangulated as P_1, P_2 as in [2]. The gluings for said pillow are given in Table

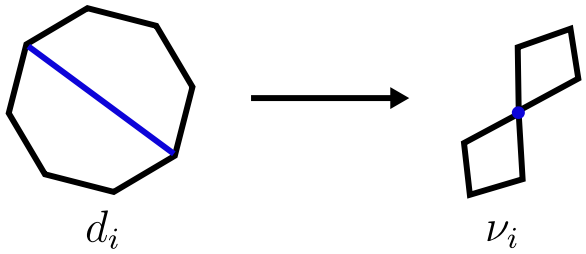


FIGURE 8. Collapsing a diagonal of d_i maps to ν_i.

1. This pillow may be added by un-gluing any face having one vertex on v_N (v_S) and another on v_K and attaching the respective P_i. After gluing P_1, P_2 we have an ideal-triangulation $\mathcal{T}^*$ of $S^3\backslash K$.

tet/face	(012)	(013)	(023)	(123)
$P_{i,0}$	$P_{i,1}(013)$	—	—	$P_{i,1}(012)$
$P_{i,1}$	$P_{i,0}(123)$	$P_{i,0}(012)$	$P_{i,1}(123)$	$P_{i,1}(023)$

TABLE 1. Triangulation of P_i, a pillow with pre-drilled tube [2].

2. Implementation

We give two implementations of the octahedral ideal-triangulation based on the five tetrahedra division of an octahedron. For a crossing of a knot diagram, there are two ways to triangulate the associated ideal-octahedron lying between the crossing strands. The two choices are shown in Figure 10. If all ideal-octahedra are triangulated according to the first choice, we call the octahedral ideal-triangulation the *meridional ideal-triangulation* $\mathcal{T}_m$; if the second choice is used we will call the octahedral ideal-triangulation the *longitudinal ideal-triangulation* $\mathcal{T}_l$. These ideal-triangulations are named according to the diagonals of the quadrilateral obtained by truncated vertices 0 and 5. In the meridional ideal-triangulation, this each diagonal is a meridional curve on $\partial N(K)$; in the longitudinal ideal-triangulation, the union of all such diagonals forms a relatively short longitudinal curve in $\partial N(K)$ which has linking number zero with K. $\mathcal{T}_m$ has found usage in relation to the colored Jones polynomial [1], and colored Khovanov homology [4], while $\mathcal{T}_l$ is particularly useful in finding minimal genus Seifert surfaces.

There are two choices for labeling the vertices of a tetrahedron, shown in Figure 9. We will use labeling (a), the *right-handed labeling*, for every tetrahedra to aid in implementation. This labeling can be thought of in the following way: position one's right hand so as to grab the edge (01) with thumb pointing towards vertex 0; the fingers of one's hand curl from vertex 3 to vertex 2.

2.1. Planar Diagram Codes.

Both implementations will rely on planar diagram codes, or *PD-codes*. PD-codes were chosen due to their read/writability as well as their inclusion in SageMath and SnapPy. Let K be a knot in S^3 and D an oriented diagram of K. Each sub-arc of D is labeled starting with the numeral 1 and labeled successively following along the knot in accordance with the orientation. At each

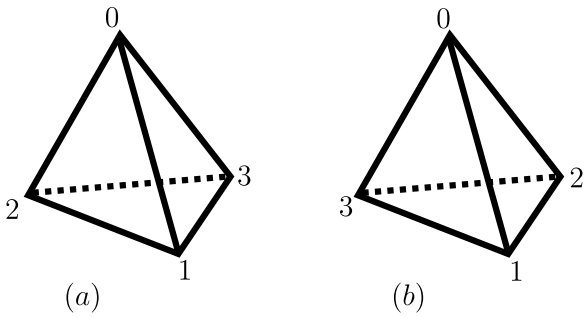


FIGURE 9. The right- (a) and left- (b) handed labelings of the vertices of a tetrahedron.

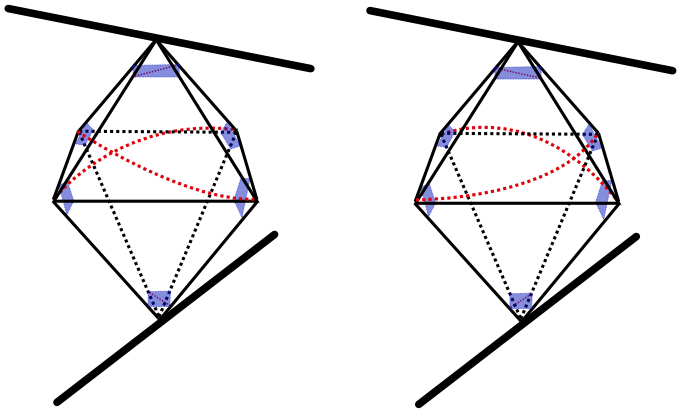


FIGURE 10. The choices of triangulating an ideal-octahedron that yields $\mathcal{T}_m$ and $\mathcal{T}_l$ respectively.

crossing a 4-tuple is recorded called the *crossing code*. Beginning with the incoming under-arc and reading counter-clockwise the arc labels are recorded. See Figure 11.

With a single exception, the orientation of a crossing can be determined from a crossing code by examining the 2nd and 4th entries. If the second entry is the successor of the fourth entry modulo $2C$ where C is the number of crossings, then the crossing is right-handed. If the fourth entry is the successor of the second entry modulo $2C$, then the crossing is left-handed. The exception to this are one-crossing diagrams of the unknot shown in Figure 12.

Remark 2.1. Another convention for PD-codes is to begin at the incoming over-arc. If such a code is read via our convention, then the resulting knot will be the mirror.

2.2. **Meridional Ideal-Triangulation.** We give here the explicit face pairings yielding the meridional ideal-triangulation. Again, let K be a knot in S^3, D an oriented diagram of K labeled as in Section 2.1 with C crossings. At each crossing we triangulate the ideal-octahedron according to the orientation of the crossing, o^r, o^l depicted in Figure 13. Incident to the over-strand will be two tetrahedra, u_b, u_f associated to the sub-arcs $i, i+1$ of the under-strand respectively. Likewise for at the under-strand, we give l_b, l_f as the tetrahedra associated to the sub-arcs $j, j+1$ of the over-strand respectively. We write $i \to u_b, i+1 \to u_f$ *et cetera* to denote these associations. The fifth tetrahedra z sets between. Tables 2 and 3 give the triangulations of o^r and o^l.

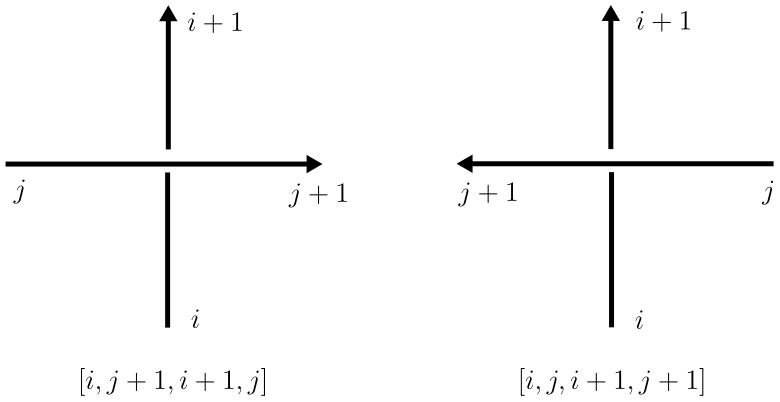


FIGURE 11. A right and a left hand crossing and their corresponding codes.

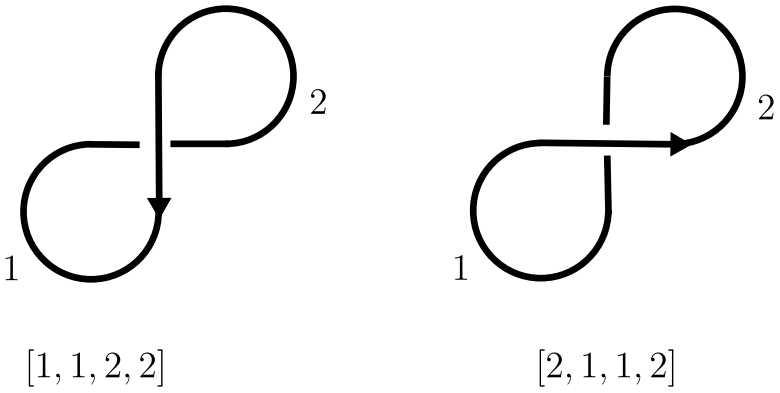


FIGURE 12. Two diagrams of the unknot in which the orientation of the crossing code is not determined by the 2nd and 4th entries.

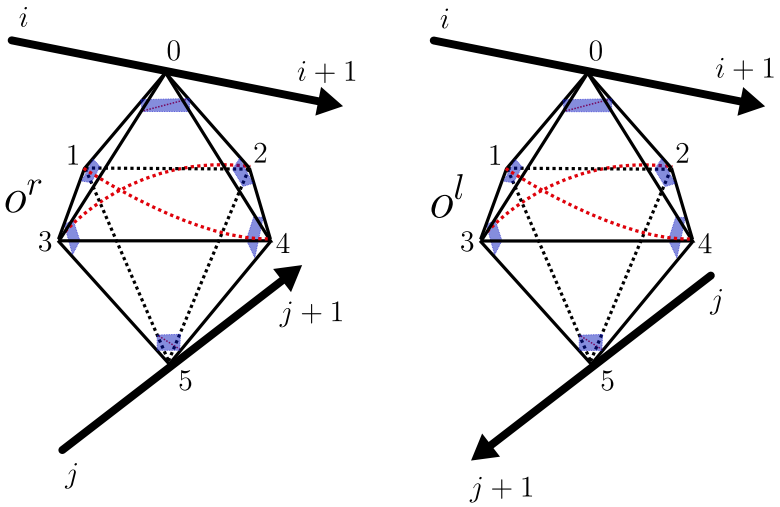


FIGURE 13. The two ideal-octahedra o^r and o^l with sub-arc labeled.

For every integer $1 \leq i \leq 2C$ there is exactly one of u_f, l_f and one of u'_b, l'_b associated to the sub-arc labeled i (it is possible for u_f, l_f to belong to the same octahedron as u'_b, l'_b). The face pairings described in Section 1 of the twisted octahedra induce face

tet/face	(012)	(013)	(023)	(123)
$u_b = o^r(0123)$	$z(320)$	$u_f(012)$	—	—
$u_f = o^r(0234)$	$u_b(013)$	$z(321)$	—	—
$z = o^r(1234)$	$l_f(013)$	$l_b(012)$	$u_b(210)$	$u_f(310)$
$l_b = o^r(1345)$	$z(013)$	$l_f(012)$	—	—
$l_f = o^r(1245)$	$l_b(013)$	$z(012)$	—	—

TABLE 2. Triangulation of o^r. Tetrahedra u_b, u_f, l_b, l_f are associated with the sub-arcs $i, i+1, j, j+1$ respectively.

tet/face	(012)	(013)	(023)	(123)
$u_b = o^l(0123)$	$z(320)$	$u_f(012)$	—	—
$u_f = o^l(0234)$	$u_b(013)$	$z(321)$	—	—
$z = o^l(1234)$	$l_b(102)$	$l_f(103)$	$u_b(210)$	$u_f(310)$
$l_b = o^l(1245)$	$z(102)$	$l_f(012)$	—	—
$l_f = o^l(1345)$	$l_b(013)$	$z(103)$	—	—

TABLE 3. Triangulation of o^l. Tetrahedra u_b, u_f, l_b, l_f are associated with the sub-arcs $i, i+1, j, j+1$ respectively. Note the changes in l_b, l_f.

pairings on the ideal-tetrahedra associated to i given by the following map ϕ:

$$\phi(i) = \begin{cases} u_f(023) \to u'_b(032), u_f(123) \to u'_b(132) & ; i \to u_f, u'_b \\ u_f(023) \to l'_b(231), u_f(123) \to l'_b(230) & ; i \to u_f, l'_b \\ l_f(023) \to u'_b(231), l_f(123) \to u'_b(230) & ; i \to l_f, u'_b \\ l_f(023) \to l'_b(032), l_f(123) \to l'_b(132) & ; i \to l_f, l'_b \end{cases} \tag{2.1}$$

Algorithm 2.2. Given a PD-code, for each crossing code c_i, generate the appropriate ideal-octahedron o_i^r or o_i^l. For each integer $1 \leq k \leq 2C$, k appears exactly twice amongst all crossing codes, say in c_i, c_j (possible $i = j$). The positions of k in c_i, c_j determine the associated ideal-tetrahedra. It is then possible to determine the map $\phi(k)$. After applying $\phi(k)$ for each $1 \leq k \leq 2C$, the ideal-triangulation $\mathcal{T}$ of $(S^2 \times I) \backslash K$ has been generated. Finally, add the pillows with pre-drilled tubes P_1, P_2 at the faces $u_f(023), l_f(023)$ of o_1 successively. This yields the desired octahedral ideal-triangulation $\mathcal{T}_m$ of $S^3 \backslash K$.

Example 2.3. We construct an octahedral ideal-triangulation for the complement of the unknot given by the diagram on the left of Figure 12. The PD-code is $[[1, 1, 2, 2]]$, and based on the diagram the crossing is right-handed. We triangulate o^r. As there is only one ideal-octahedron, u_f must be glued to l_b and l_f to u_b according to $\phi(1), \phi(2)$ respectively. This yields the following ideal-triangulation:

tet/face	(012)	(013)	(023)	(123)
u_b	$z(320)$	$u_f(012)$	$l_f(312)$	$l_f(302)$
u_f	$u_b(013)$	$z(321)$	$l_b(231)$	$l_b(230)$
z	$l_f(013)$	$l_b(012)$	$u_b(210)$	$u_f(310)$
l_b	$z(013)$	$l_f(012)$	$u_f(312)$	$u_f(302)$
l_f	$l_b(013)$	$z(012)$	$u_b(231)$	$u_b(230)$

Finally, we add the pillows with pre-drilled holes P_1, P_2 at faces $u_b(123) \leftrightarrow l_f(302)$ and $l_b(123) \leftrightarrow u_f(302)$:

tet/face	(012)	(013)	(023)	(123)
u_b	$z(320)$	$u_f(012)$	$l_f(312)$	$P_{1,0}(302)$
u_f	$u_b(013)$	$z(321)$	$P_{2,0}(013)$	$l_b(230)$
z	$l_f(013)$	$l_b(012)$	$u_b(210)$	$u_f(310)$
l_b	$z(013)$	$l_f(012)$	$u_f(312)$	$P_{2,0}(302)$
l_f	$l_b(013)$	$z(012)$	$P_{1,0}(013)$	$u_b(230)$
$P_{1,0}$	$P_{1,1}(013)$	$l_f(023)$	$u_b(231)$	$P_{1,1}(012)$
$P_{1,1}$	$P_{1,0}(123)$	$P_{1,0}(012)$	$P_{1,1}(123)$	$P_{1,1}(023)$
$P_{2,0}$	$P_{2,1}(013)$	$u_f(023)$	$l_b(231)$	$P_{2,1}(012)$
$P_{2,1}$	$P_{2,0}(123)$	$P_{2,0}(012)$	$P_{2,1}(123)$	$P_{2,1}(023)$

References

[1] ChoJinseok and MurakamiJun, "Optimistic limits of the colored jones polynomials," *Journal of the Korean Mathematical Society*, vol. 50, no. 3, pp. 641–693.

[2] J. Howie, D. Mathews, and J. Purcell, "A-polynomials, ptolemy varieties and dehn filling," 02 2020.

[3] H. Kim, S. Kim, and S. Yoon, "Octahedral developing of knot complement i: Pseudo-hyperbolic structure," *Geometriae Dedicata*, vol. 197, 12 2018.

[4] C. R. S. Lee, "Normal surfaces and colored khovanov homology," 2022. [Online]. Available: https://arxiv.org/abs/2201.13393

[5] W. Thurston, "The geometry and topology of 3-manifolds," *Lecture notes, Princeton*, 1977.